Uniport Journal of Engineering and Scientific Research (UJESR)

Vol. 8, Issue 2, 2024, Page 130-136
ISSN: 2616-1192

(www.ujesr.org)

1.2 to 1.8 GHz Surface Accoustic Wave Oscillator for Wireless Applications

Akwuruoha, C.N
Department of Electrical and Electronic Engineering, Michael Okpara University of Agriculture Umudike, Nigeria
*Corresponding author's email: akwuruoha.charles@mouau.edu.ng

Abstract
This paper presents a 1.2 to 1.8 GHz surface acoustic wave (SAW) oscillator for wireless applications. The oscillator was designed based on IBM NPN bipolar junction transistor biased with collector voltage of 10V. The SAW oscillator has a centre (fundamental) frequency of 1.5 GHz. The oscillator was subjected to large signal S-parameter simulation from 1.2 to 1.8 GHz and found to sustain oscillations across the 600 MHz bandwidth in accordance with Nyquist Criterion. Time domain analysis carried out with respect to collector voltage, collector current, dB output voltage and resonant voltage carried out indicated consistent operation of the SAW oscillator from 0 to 1.4ns. Phase and amplitude noise analysis (in dBc/KHz) carried out with respect to the output and resonant voltages showed low noise functionality of the SAW oscillator.

Keywords: *Surface acoustic wave, Oscillator, Bandwidth, bipolar junction transistor, Time domain analysis, Wireless application*

Received: 26th May, 2024 *Accepted: 17th September, 2024*

1. Introduction

The recent surge in demand for low power, high quality factor and highly sensitive applications for wireless, medical, ultrasonic, chemical and sensing operations has brought to the fore the importance of surface acoustic wave (SAW) oscillators. Oscillators generally find applications in radio frequency and microwave circuits where there is desirability to convert dc signals to ac sinusoidal signals thereby minimizing unwanted harmonics and noise sidebands (Gonzalez, 2007). Surface acoustic wave oscillators find application in a wide range of areas such as mobile wireless communications (Calle et al., 2005; Nimal et al., 2006; Wright, 1989). Nitride-based surface acoustic wave ultrasonics (Yantchevet al, 2002), sensors (Lee et al., 2008; Mitsakakis et al., 2009; Morgan, 2003; Rácz et al., 2011; Rocha-Gaso et al., 2009; Thomas et al., 2012) and chemical processes (Stier et al., 1998). Surface acoustic wave oscillators have been designed with gallium nitride (Campbell, 1998; Jeong et al., 2001; Nishimura et al., 2005) and gallium arsenide (Baca et al., 1999). Integrated circuit surface acoustic wave oscillators have also been reported (Avramov et al., 2009; Heller et al., 2009). Low power surface acoustic devices were reported by Elbarkouky et al. (2007). Surface acoustic wave oscillators are reportedly driven by low power. Surface acoustic wave oscillators require high quality factor (Q) resonators. High Q surface acoustic wave resonators have been reported in some works (Avramov, 2006; Hartmann, 1992; Kimura et al, 2010; Kshetrimayum et al., 2011). This is the first reported SAW oscillator operating from 1.2 to 1.8 GHz and centred at 1.5 GHz.

2. Theory

The oscillator can be described as linear feedback circuit on a transistor amplifier with gain G having an input voltage V_{in} and an output voltage V_{out} as well as a frequency-dependent feedback network with transfer function H at a frequency ω as shown in Fig. 1 (Pozar, 2011).

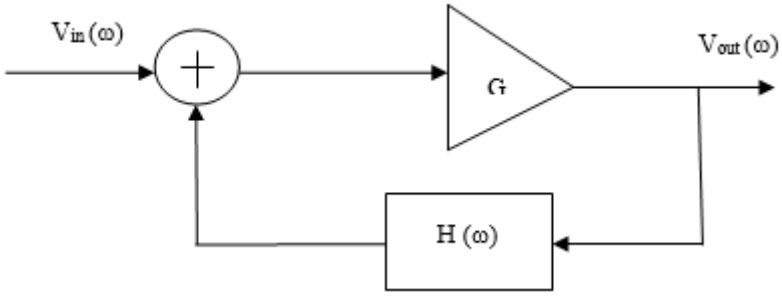

Fig. 1: Block diagram of an RF oscillator with frequency dependent feedback circuit

The output voltage V_{out} (ω) is given by Equation (1) (Pozar, 2011)

$$V_{out}(\omega) = G\,V_{in} + H(\omega)\,G\,V_{out} \quad (1)$$

Solving Equation (1) gives V_{out} (ω) in terms of V_{in} (ω) as

$$V_{out}(\omega) = GV_{in}(\omega)/(1-GH(\omega)) \quad (2)$$

Oscillation results in Equation (2) is achieved in accordance with Nyquist even at zero input voltage. Oscillators can be divided into two classes in accordance with the transistor device used in the oscillator design either as bipolar junction transistor oscillator or field effect transistor oscillator (Pozar, 2011). In this paper, bipolar junction transistor oscillator is proposed. The block diagram of a two-port transistor oscillator consisting of the terminating network, transistor with S-parameters [S] and load network is shown in Fig. 2. Γ_s and Z_s are the respective source reflection coefficient and source impedance facing the terminating network. Γ_{in} and Z_{in} are the input reflection coefficient and input impedance respectively facing port 1. Γ_{out} and Z_{out} are the output reflection coefficient and output impedance respectively facing port 2. Γ_L and Z_L are the respective load reflection coefficient and load impedance facing the load network.

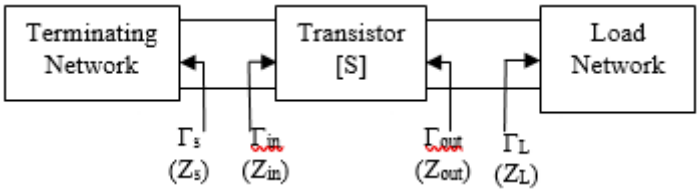

Fig. 2: Transistor oscillator block diagram

The terminating impedance Z_s is given by Equation (3):

$$Z_s = R_s + jX_s \quad (3)$$

where Z_s is the source impedance, R_s is the source resistance and X_s is the source reactance. The terminating (load) impedance Z_L is chosen to match with the input impedance (Z_{in}) herein referred to as the input reactance (X_{in}). Although it is desirable to use large signal s-parameters, if small signal s-parameters is used whereby R_s is chosen such that:

$$R_s = R_{in} + jX_{in} < 0 \quad (4)$$

There is need to reduce the power available to source as an increase in power available to the source can result in gradual increase in R_{in} such that the circuit will no longer oscillate as the oscillator tends to become stable under the condition represented by Equation (5):

$$R_{in} + jX_{in} > 0 \quad (5)$$

To ensure that oscillation occurs, the reactive part of source impedance must be chosen such that at oscillation, the circuit resonates at:

$$X_s = -X_{in} \quad (6)$$

In addition, it is desirable to have oscillation between the oscillator terminating network and the input port of the transistor simultaneously as the output port of the transistor. A steady state oscillation is achieved at the transistor input port when:

$$\Gamma_s\Gamma_{in} = 1 \quad (7)$$

such that:

$$1/\Gamma_s = \Gamma_{in} \quad (8)$$

where Γ_s and Γ_{in} are the source and input reflection coefficients respectively.

$$\Gamma_{in} = S_{11} + [(S_{12}S_{21}\Gamma_L) / (1-S_{22}\Gamma_L)] \quad (9)$$

$$\Gamma_{in} = [(S_{11}-\Delta\Gamma_L) / (1-S_{22}\Gamma_L)] \quad (10)$$

where $\Delta = S_{11}S_{22} - S_{12}S_{21}$

S_{11} is the input return loss, S_{22} is the output return loss, S_{21} is the forward transmission coefficient, S_{12} is the reverse transmission coefficient. The load reflection coefficient is given by Equation (11):

$$\Gamma_L = (1-S_{11}\Gamma_s) / (S_{22}-\Delta\Gamma_s) \quad (11)$$

The output reflection coefficient is therefore given by Equation (12):

$$\Gamma_{out} = S_{22} + [(S_{12}S_{21}\Gamma_s)/(1-S_{11}\Gamma_s)] = (S_{22}-\Delta\Gamma_s)/(1-S_{11}\Gamma_s) \quad (12)$$

3. Saw oscillator design

The surface acoustic wave oscillator consists of the resonant circuit (resonator) connected to the core oscillator (main circuit) via an oscillator port to the oscillator circuit. The schematic circuit showing the resonator and core oscillator sections of the SAW oscillator is shown in Fig. 3. The core oscillator circuit is a feedback amplifier circuit. The oscillator port has an impedance of 21Ω. The three-element resonator has series inductor (L_1) and capacitor (C_1) in parallel with a capacitor (C_2). The amplifier circuit contains blocking capacitors C_3 and C_4 of 0.1pF and 5pF, respectively. The amplifier circuit was designed based on IBM NPN transistor biased with collector voltage of 10V through a 200nH inductor. Resistors R_1 and R_2 connected to the base of the transistor have values of 4kΩ and 2kΩ respectively while the emitter is shunted by a 300 Ω resistor. The SAW oscillator output is terminated with a 20Ω load resistor (R_L). The cut off frequency of the oscillator stands at 1.5 GHz.

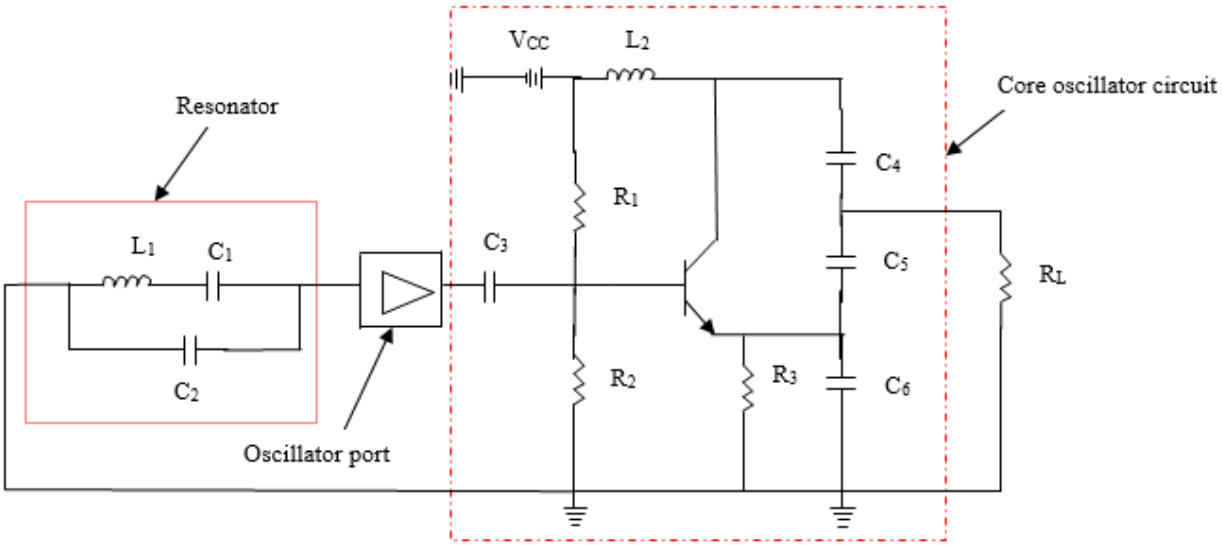

Fig. 3: SAW oscillator schematic circuit

4. Results and discussion

4.1 dB Output and Resonance voltage and time domain analysis

One-Tone harmonic balance simulation was carried out at 1.5 GHz centre frequency and 10V collector biasing voltage to achieve large signal oscillations. The voltage spectra from dc to 11 GHz is shown in Fig. 4. The dB voltage spectra indicates that at 1.5 GHz frequency, the dB voltage at output and resonance stand at -7.8 dB and 6.5 dB

respectively while at 10.6 GHz, the dB output voltage is -42.5 dB while the dB resonance voltage stands at -21.8 dB. The time domain analysis graph is shown in Fig. 5 whereby, the analysis carried out from 0 to 1.4ns and specifically taken at 0.7ns indicates that at 0.7ns, the output voltage is 0.3 V as the resonance voltage is 2.1 V.

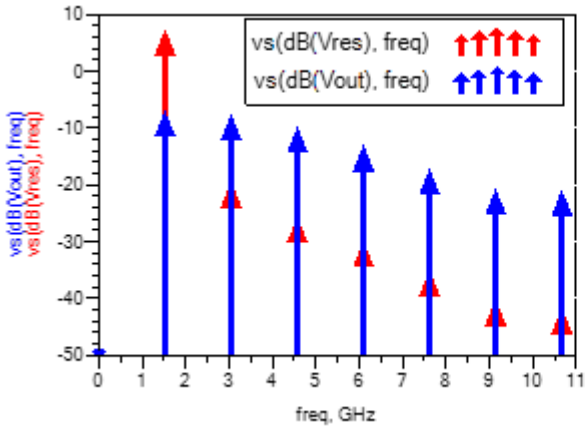

Fig. 4: Output and resonance voltage

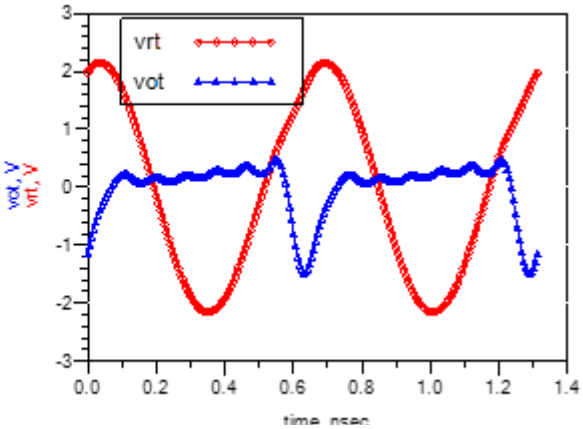

Fig. 5: Output voltage and resonance voltage time domain analysis

4.2 Phase and amplitude noise at resonance voltage ($V_{res,pnmx}$ and $V_{res,\ anmx}$)and output voltage (($V_{out,pnmx}$ and $V_{out,\ anmx}$)

Single frequency non-linear phase noise analysis was carried out at centre frequency of 1.5 GHz at dynamic range of 15. The oscillator port has a characteristic impedance of 21Ω. Harmonic balance simulation swept from non-linear noise of 10 Hz to 1 MHz at collector voltage of 10V is shown in Fig. 6 and 7. The phase noise (in dBc) is denoted by pnmx while the amplitude noise (in dBc) is denoted by anmx. The amplitude and phase noise at output voltage ($V_{out,anmx}$ and $V_{out,pnmx}$) and resonance voltage ($V_{res,anmx}$ and $V_{res,pnmx}$) are examined at 10Hz, 1KHz and 1 MHz, respectively. The phase and amplitude noise for output voltage and resonance voltage are shown in Fig. 6. The output voltage phase noise and amplitude noise are as follows: for 10 Hz are -46.3 and -93.5dBc, for 1 KHz are -91.8 dBc and -138.9 dBc for 1 MHz are -162.9 dBc and -166.0 dBc. The resonance voltage phase and amplitude noise are shown in Fig. 7. The phase noise and amplitude noise are as follows: for 10 Hz are -91.8 dBc and -136.3 dBc, for 1 KHz are -46.3 dBc and -90.9 dBc, for 1 MHz are -162.5 dBc and -165.3 dBc.

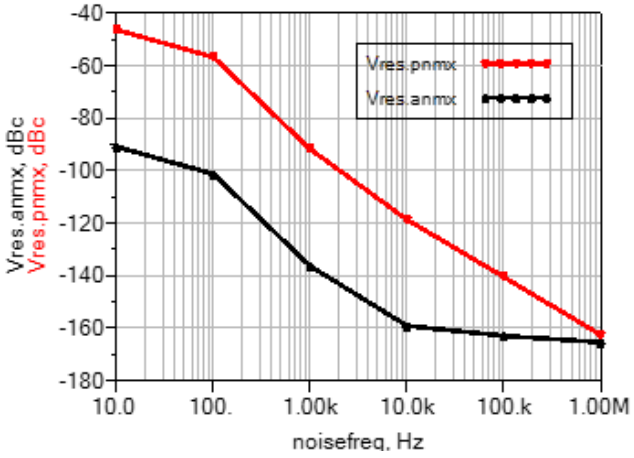

Fig. 6: Amplitude and phase noise at resonance

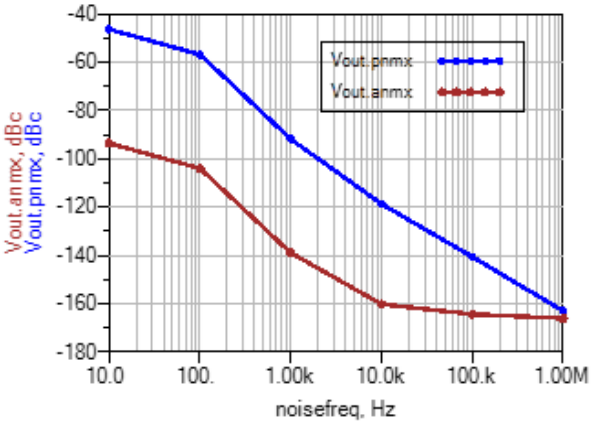

Fig. 7: Amplitude and phase noise at output voltage

4.3 Time domain collector voltage (V_{CE}) and collector current (I_C)

Time domain analysis of the SAW oscillator was carried out with respect to the collector-emitter

voltage (V_{CE}) and collector current (I_C) between 0 to 1.4 ns (nano seconds) during large signal dc simulation. The results indicates that the collector-emitter voltage has a peak value of 7.3 V at 0.45 ns and the least value of 4.4V at 0.64 ns as shown in Fig. 8. The collector current result is shown in Fig. 9 whereby the peak collector current stood at 0.08 mA at 0.63 ns as the least collector current stood at 0.01 mA at 0.54 ns. The superimposed large signal dc V_{CE} and I_C characteristics are shown in Figure10 which indicates that at collector-emitter voltage of 6.3V the collector current stood at 0.02mA.

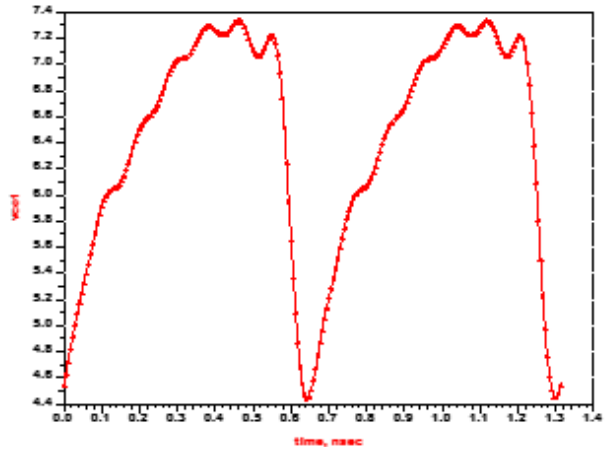

Fig. 8: Collector-emitter voltage (V_{CE}) versus

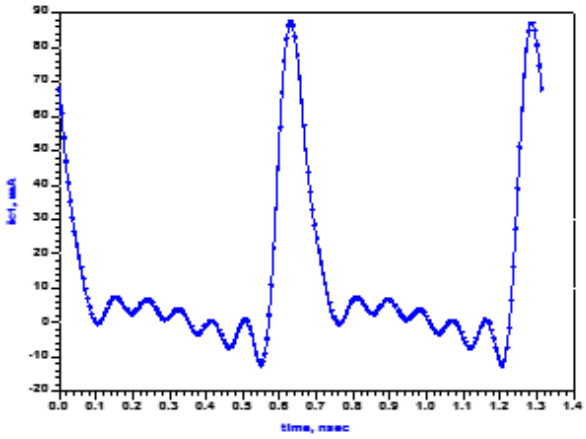

Fig. 9: Collector current (I_C) versus time

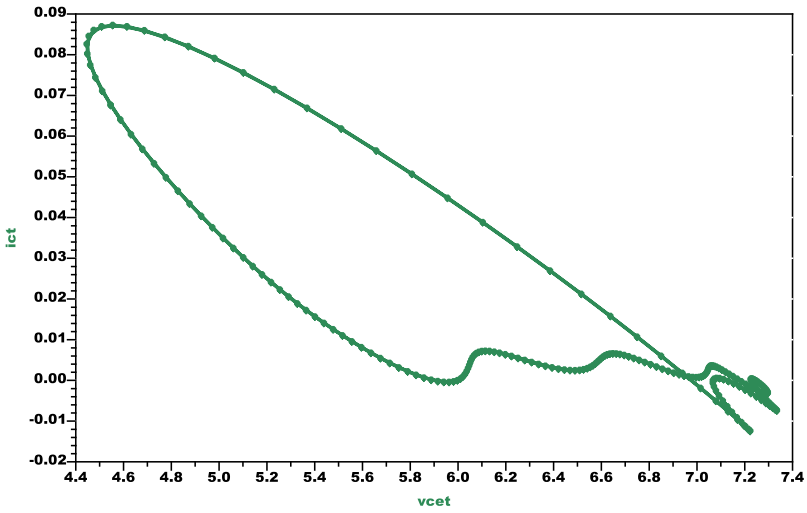

Fig. 10: Superimposed collector current (I_C) versus collector-emitter voltage (V_{CE})

4.4 Oscillation test

The oscillator was tested for oscillation (instability) at characteristic impedance of 13.5Ω from 1.2 GHz to 1.8 GHz as shown by Fig. 11 and 12. In Fig. 11, the magnitude and phase of the input return loss (S_{11}) at 1.53 GHz was found to be 1.02 while the phase stood at 178.9. This is an indication of oscillation and the desired instability by the SAW oscillator. The Oscillation and instability were confirmed by Nyquist stability criterion polar plot shown in Fig. 12 whereby the oscillator is considered oscillating if the Nyquist loop (S_{11}) encircles the point 1+j*0, moving in the clockwise direction with respect to increasing frequency from 1.2 to 1.8 GHz.

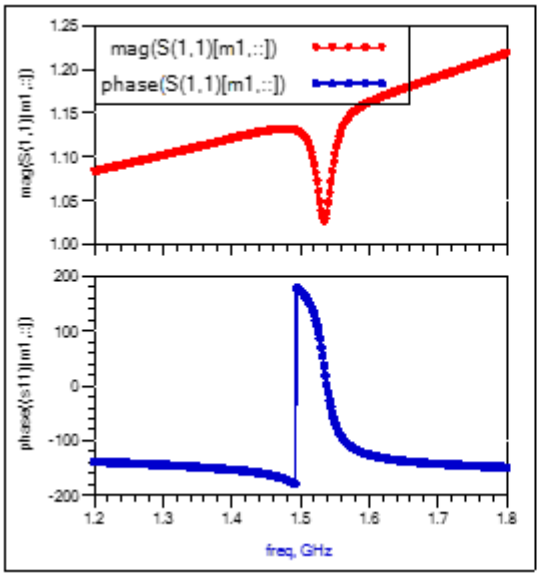

Fig. 11: Magnitude and Phase of input return loss

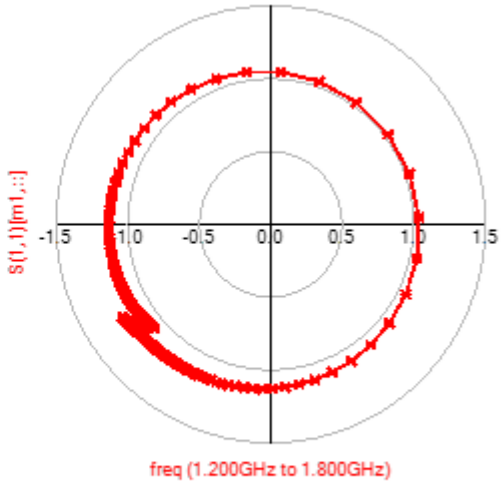

Fig. 12: Nyquist loop from 1.2 to 1.8 GHz

5. Conclusion

A 1.2 to 1.8 GHz surface acoustic wave oscillator with centre frequency of 1.5 GHz has been proposed, designed and simulated. The oscillator sustained oscillation across the entire bandwidth of 600 MHz. The SAW oscillator will find application in wireless, ultrasonic and sensing applications where there is desirability for low voltage and low power.

Acknowledgement

The Author is grateful to IBM USA.

References

Avramov, I.D. (2006) Design of Rayleigh SAW Resonators for Applications as Gas Sensors in Highly Reactive Chemical Environments. IEEE International Frequency Control Symposium and Exposition, 381–388.

Avramov, I., Arapan, L., Katardjiev, I., Strashilov, V. and Yantchev, V. (2009) IC-compatible power oscillators using Thin Film Plate Acoustic Resonators (FPAR). Proceedings of IEEE International Ultrasonics Symposium, 855-858.

Baca, A.G., Heller, E.J., Hietala, V.M., Casalnuovo, S.A., Frye-Mason, G.C., Klem, J.F. and Drummond, T.J. (1999) Development of a GaAs monolithic surface acoustic wave integrated circuit. IEEE Journal of Solid-State Circuits, 34: 1254-1258.

Calle, F., Peds, J., Palacios, T. and Grajal, J. (2005) Nitride-based surface acoustic wave devices and applications. Physica Status Solidi, 2: 976-983.

Campbell, C.K. (1998) Surface Acoustic Wave Devices for Mobile and Wireless Communications, Academic Press, 9(8).

ElBarkouky, M., Wambacq, P. and Rolain, Y. (2007) A low-power 6.3 GHz FBAR overtone-based oscillator in 90 nm CMOS technology. Microelectronics and Electronics Conference, 61-64.

Gonzalez, G. (2007) Foundations of Oscillator Circuit Design, Artech House, USA.

Hartmann, C.S., Chen, D.P. and Heighway, J. (1992) Modelling of SAW transversely coupled resonators filters using coupling of-modes modelling technique. Proceedings of Ultrasonics Symposium, 39–44.

Jeong, H.H., Kim, S.K., Lee, J.S., Choi, H.C., Lee, J.H. and Lee, Y.H. (2001) Investigation of dopant dependent wave velocity in GaN thin film SAW filter. Proceedings of IEEE Ultrasonics Symposium, 207-209.

Kimura, T., Kadota, M. and Ida, Y. (2010) High Q SAW resonator using upper-electrodes on grooved-electrodes in LiTa03. IEEE MTT-S International Microwave Symposium Digest, 1740-1743.

Kshetrimayum, R., Yadava, R.D.S. and Tandon, R.P. (2011) Modelling electrical response of polymer-coated SAW resonators by equivalent circuit representation. Ultrasonics, 51(5): 547–553.

Lee, C.M., Wong, K.M., Chen, P. and Lau, K.M. (2008) GaN based lamb-wave mass-sensors on silicon substrates. Proceedings of IEEE

International Ultrasonic Sensors Symposium, 2008-2011.

Mitsakakis, K., Tserepi, A. and Gizeli, E. (2009) SAW device integrated with microfluidics for array-type biosensing. Microelectronic Engineering, 86(4-6): 1416–1418.

Morgan, D.P. (2003) Simplified analysis of surface acoustic wave one-port resonators. Electronics Letters, 39(18): 4–5.

Nimal, A.T., Singh, M., Mittal, U. and Yadava, R.D.S. (2006) A comparative analysis of one-port Colpitt and two-port Pierce SAW oscillators for DMMP vapor sensing. Sensors and Actuators B: Chemical, 114(1): 316– 325.

Nishimura, K., Slligekawa, N., Yokoyama, H., Hiroki, M., & Hollkawa, K. (2005) SAW characteristics of GaN layers with surfaces exposed by dry etching. IEICE Electronics Express, 2: 501-505.

Pozar, D.M. (2011) Microwave Engineering. Fourth edition, John Wiley & Sons Incorporation, USA.

Rácz, Z., Cole, M., Gardner, J.W., Pathak, S., Jordan, M.D. and Challiss, R.A.J. (2011) Cell-Based Surface Acoustic Wave Resonant Microsensor for Biomolecular Agent Detection. 16th International Conference on Solid-State Sensors, Actuators and Microsystems, 2168-2171.

Rocha-Gaso, M.I., March-Iborra, C., Montoya-Baides, A. and Arnau-Vives, A. (2009) Surface Generated Acoustic Wave Biosensors for the Detection of Pathogens: A Review. Sensors, 9(12): 5740–5769.

Stier, S., Voigt, A., Rapp, M., Gmbh, F.K., Box, P.O. and Karlsruhe, D. (1998) Influence of Phase Position on the Performance of Chemical Sensors Based on SAW Device oscillators. Analytical Chemistry, 70(24): 5190–5197.

Thomas, S., Leong, S.L.T., Rácz, Z., Cole, M. and Gardner, J.W. (2012) Design and Implementation of a High-Frequency Surface Acoustic Wave Sensor Array for Pheromone Detection in an Insect-inspired Info-chemical Communication System. 14th International Meeting on Chemical Sensors, 11–14.

Wright, P.V. (1989) Analysis and design of low-loss SAW devices with internal reflections using coupling-of-modes theory. Proceedings of IEEE Ultrasonics Symposium, 141–152.

Yantchev, V.M., Member, S., Strashilov, V.L., Rapp, M., Stahl, U. and Avramov, I.D. (2002) Theoreticaland Experimental Mass-Sensitivity Analysis of Polymer-Coated SAW and STW Resonators for Gas Sensing Applications. IEEE Sensors Journal, 2(4): 307–313.